Domed and Released Thin-Film Construct—An Approach for Material Characterization and Compliant Interconnects

Gregory T. Ostrowicki, Nathan T. Fritz, Raphael I. Okereke, Paul A. Kohl, *Member, IEEE*, and Suresh K. Sitaraman

***Abstract*—An approach for microfabricating precisely defined spherical 3-D domes through a simple low-temperature polymer reflow process was developed. Release of a thin metal film patterned over the domed structure was accomplished by the removal of the underlying polymer using two different methods: dry thermal decomposition and wet supercritical release. The domed shape impacted the effect of stiction during the release step and assisted in the release of large millimeter-size film geometries. The dome and release procedures were used to fabricate an experimental test specimen that functions as either a tensile or interfacial fracture test for thin films on rigid substrates. Other potential applications of the domed metal structures such as compliant electrical interconnects are discussed.**

***Index Terms*—Compliant interconnects, delamination, dome, MEMS, reflow, stiction, tensile test, thin film.**

I. Introduction

MICROELECTRONIC and MEMS fabrication typically involves a set of serially processed 2-D layers, resulting in a final structure that is either flat or mildly terraced. More complicated 3-D shapes, such as angular pyramids and valleys, usually require selective etching along crystal planes in single crystalline substrates. These wet or dry chemical etching processes can be fabrication intensive with resulting geometries that are highly sensitive to process parameters. Thus, there is a continuing need to develop microfabrication techniques that enable the formation of 3-D geometries for next-generation MEMS and microelectronic devices.

A particularly simple and useful shape for MEMS designs is the spherical dome or cylindrical strip. Several schemes for fabricating these shapes have been developed. Some dome-shaped features have been cast from prefabricated molds with concave cavities. For example, PMMA microlenses were cast from an isotropically etched silicon mold [1]. Machined metal spheres or reflowed solder lines have also been used as stamps to create domed depressions into soft materials [2], [3]. In addition, these cavities can be coated with structural material which upon etching of the mold results in a dome-shaped membrane [2], [4], [5]. These fabrication techniques however can be rather complex and may not be appropriate for applications requiring a simple dome shape on a substrate surface. A promising method for such a bottom–up approach to dome formation relies on thermal reflow of patterned flat materials. While reflow of solder is well known to result in spherical profiles, recent work in the reflow of polymer photoresists allows for simple low-temperature dome fabrication [6], [7]. These photoresist domes are ideal sacrificial materials as they are easily both patterned and removed. However, the thermal reflow process often requires several bake steps to prevent bubble formation and acetone vapor pretreatment to aid in reflow uniformity, and the final geometry is dependent on several factors, including reflow time, acetone vapor concentration, and aspect ratio of the original photoresist feature [8]. An alternative to the traditional photoresist dome is the fabrication of air-filled domes through the thermal decomposition of a photodefinable polymer. These thermally developed photoresists decompose into gas when heated and diffuse through the encapsulating membrane, and can result in air-filled domes under the right conditions [9].

In this paper, we present a straightforward methodology of fabricating spherical domed structures using a thermally developed polymer and a one-step reflow process. This technique has several advantages over conventional polymer dome formation, including the following: no vapor pretreatment, one low-temperature bake step, fully formed domes in minutes, precisely defined footprint and curvature, and robust processing. Furthermore, the reflowable polymer can be spin coated, is photodefinable, is developed by a dry thermal process, and can be removed via either thermal decomposition or wet solvent etch. The use of these polymer domes as a sacrificial supporting structure was demonstrated by the fabrication of test specimens for a novel thin-film material characterization experiment. The test specimens featured an electrodeposited and patterned metal film over the dome which was released after the removal of the reflowed photoresist. There was significant learning through the iterative fabrication development process of the proposed thin-film test, particularly regarding strategies for avoiding stiction when releasing large millimeter-sized metal films over reflowed polymer domes. In the following sections of this paper, we describe the procedure for fabricating precisely defined domes, extend the fabrication to create a compliant metal structure for a thin-film characterization application, cover dry and wet

Manuscript received 6, 2011; revised August 24, 2011; accepted October 7, 2011. Date of publication December 6, 2011; date of current version March 7, 2012. This work was supported by the National Science Foundation under Grants CMMI-0800037 and ECCS-0901679.

G. T. Ostrowicki, R. I. Okereke, and S. K. Sitaraman are with the George W. Woodruff School of Mechanical Engineering, Georgia Institute of Technology, Atlanta, GA 30332 USA (e-mail: gtostrowicki@gatech.edu; suresh.sitaraman@me.gatech.edu).

N. T. Fritz and P. A. Kohl are with the School of Chemical and Biomolecular Engineering, Georgia Institute of Technology, Atlanta, GA 30332 USA.

Color versions of one or more of the figures in this paper are available online at http://ieeexplore.ieee.org.

Digital Object Identifier 10.1109/TDMR.2011.2175927

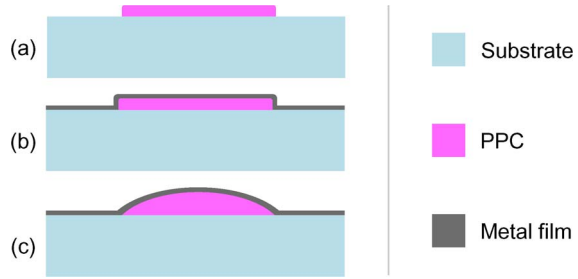

Fig. 1. Fabrication of reflowed polymer domes. (a) PPC patterning. (b) Blanket sputtered metal film. (c) Reflowed PPC on a hot plate into dome shape.

polymer removal techniques, and discuss other potential applications for the released metal structure.

II. Fabrication of Domes

A. Photolithography of Thermally Decomposable Polymer

The proposed procedure for dome fabrication begins with patterning a reflowable photoresist into flat circular shapes as in Fig. 1(a). A polypropylene carbonate (PPC)-based photoresist was formulated and used in this work. PPC and similar polymers have been studied previously for a number of temporary place holder applications in microelectronics [9]–[13]. However, these applications did not employ the technique demonstrated here for the precise definition of domed metal structures. Unlike conventional aqueous developed photoresists, PPC is developed thermally. In the particular formulation used, the native PPC decomposes into gas at temperatures above ∼150 °C. After exposure to deep UV radiation (248 nm), the decomposition temperature drops to ∼100 °C and thus allows for positive-tone imaging by subsequent heating to 100 °C–150 °C.

PPC synthesized by Novomer, Inc., was diluted into *gamma*-Butyrolactone (GBL) for a 20 wt% polymer loading. A 3% by weight of polymer photoacid generator (PAG) was added to make the formulation photosensitive. When exposed, the PAG releases an acid that decomposes the PPC into small volatile organic compounds when heated above ∼80 °C. The formulation was spin coated onto a bare silicon wafer at 3600 r/min to a thickness of 3 μm. Deep UV exposure through a photolithography mask and subsequent heating to 110 °C on a hot plate resulted in patterned disks with diameters of 2190, 2680, and 3670 μm. The remaining unexposed PPC is stable in isopropyl alcohol (IPA), and thus, an IPA wash removed any residue left by the exposed photoresist. The patterned PPC disks were then subjected to a flood exposure. The impact of this final exposure step on reflow and decomposition is discussed in the following sections.

B. Metal Film Encapsulation

The strategy for forming precisely defined domes involves encapsulating the photoresist within a thin flexible membrane in order to confine the volume in which the polymer can reflow. Three different metal films (copper, aluminum, and titanium) were sputter deposited onto some of the patterned PPC samples, both the exposed and unexposed [see Fig. 1(b)]. A Denton Vacuum Discovery dc sputterer was used to deposit 500 nm of each metal at relatively modest rates (∼10 nm/min) in order to prevent substrate heating above the reflow or decomposition temperature of PPC. Metal deposition conditions were designed to have a uniform thickness and produce a crack-free film.

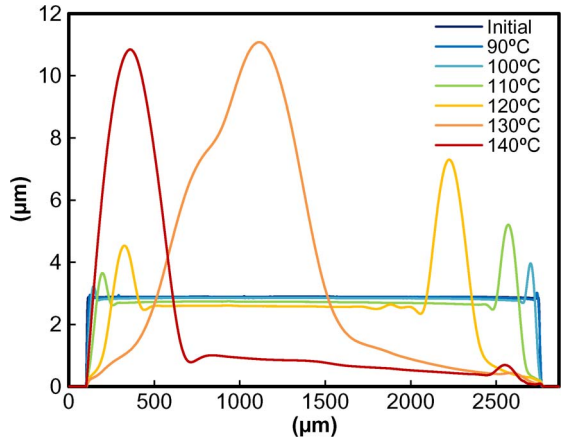

Fig. 2. Reflow of bare unexposed PPC. Profiles correspond to 10 min of heating at each incrementally increasing hot-plate temperature.

C. Reflow Characterization and Results

Reflow characterization experiments were conducted to determine the effects of flood exposure and metal coating on the fabricated PPC disks. Four sample sets were considered: bare unexposed PPC, bare exposed PPC, Cu-coated unexposed PPC, and Cu-coated exposed PPC. Samples were placed on a hot-plate set to a series of increasing temperatures from 60 °C to 140 °C in increments of 10 °C. Scanning profiles tracking the reflow progress of PPC were taken after 10 min at each bake temperature.

Bare unexposed PPC was observed to reflow above 90 °C but resulted in highly asymmetrical domelike profiles. The typical reflow progression for this case started with highly elevated edge beads that coalesced into a large off-center mound (see Fig. 2). Also, surface tension caused the outer diameter to shrink inward during reflow, and decomposition of the unexposed PPC was observed to occur at 140 °C. Bare exposed PPC, on the other hand, began to decompose above 70 °C before reflow could be observed. The Cu-coated unexposed PPC was not observed to reflow or decompose at all for the entire temperature range tested. Conversely, Cu-coated exposed PPC reflowed above 70 °C into perfectly spherical domes [see Fig. 1(c)], with no decomposition apparent for temperatures up to 120 °C. Above this temperature, some samples developed a large protruding bubble indicating significant decomposition of PPC within the dome.

For practical dome fabrication, the metal-coated exposed PPC should be baked at a constant temperature of ∼100 °C, high enough for rapid reflow yet low enough to prevent the risk of decomposition. The evolution of the dome shape at this temperature is shown in Fig. 3 and indicates a fully formed dome within less than 4 min with no change in curvature for as long as 10 min. An analytically derived profile of a constant

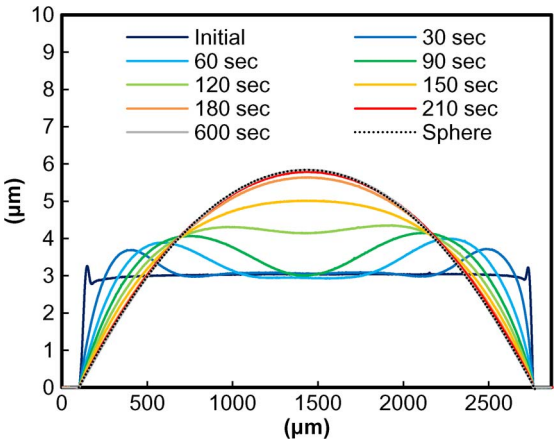

Fig. 3. Reflow of exposed PPC encapsulated by 500 nm of Cu. Profiles correspond to the amount of time that the sample spent on 100 °C hot plate. The stabilized dome matches a spherical cap with a radius of curvature $R = 15.4$ cm.

curvature dome is overlayed to show that the stabilized profile is a perfect spherical cap. Images of the encapsulated PPC before and after reflow were taken with both an optical microscope and an optical profiler as shown in Fig. 4.

The difference in behavior between the bare and sputter-coated PPC samples is believed to be attributable to a hermetic sealant effect, where the encapsulated PPC experiences elevated pressure when heated, and thus, the characteristic reflow and decomposition shifts to a higher temperature. During reflow, a spherical dome should therefore naturally form in order to equalize the pressure contained within a flexible membrane. The volume of the encapsulated PPC was measured to remain constant before and after doming, indicating no phase change during reflow. Domes were also fabricated in the same manner using Al and Ti encapsulants with similar reflow progressions, supporting the claim that the encapsulation effect and not a chemical reaction with the metal coating is responsible for the difference in PPC reflow and decomposition. The Al-, Ti-, and Cu-coated dome shapes were indistinguishable except for the color of the encapsulating metal film, and therefore, only images of Cu/PPC samples are shown in this paper for brevity.

A significant advantage of reflowing the sacrificial polymer within an encapsulant is that the lateral dimensions of the dome are precisely defined. Even with the relatively weak adhesion of Cu to Si, the outer diameter of the PPC did not change after reflow. Also, the final curvature of the dome stabilizes after only a few minutes of heating. Thus, the height and curvature of a reflowed dome can be simply determined by equating the volume of the initial PPC disk to that of a spherical cap of equivalent base diameter using

$$V = \frac{\pi}{6} h_f (3r^2 + h_f^2) \tag{1}$$

$$R = \frac{r^2 + h_f^2}{2h_f} \tag{2}$$

where V is the spherical cap volume, h_f is the dome height, r is the base radius, and R is the radius of curvature. It should be noted that the initial profile of the Cu/PPC disk before reflow as shown in Fig. 3 contains a slightly sloped sidewall and edge bead. Thus, the volume of the initial disk was found to be about 3%–5% less than that calculated using $\pi r^2 h$. When designing for specific dome dimensions by this conservation of volume approach, it is therefore important to account for this difference when choosing the appropriate dimensions of the encapsulated PPC disk. The dimensions of the fabricated reflowed domes are summarized in Table I. The three different dome diameters were chosen to accommodate different released film strip lengths as explained later in this paper. Also of note is that, for the low-profile domes fabricated in this work, a parabolic profile is virtually indistinguishable from a spherical one, and thus, determining the curvature shape of other aspect ratio domes is part of our ongoing study.

III. Thin-Film Material Characterization Test

An important potential application for reflowed PPC domes is to act as a supporting structure for subsequently defined curved 3-D features. In this paper, we demonstrate the ability to metallize, pattern, and release a compliant metal film over a dome. The geometry and fabrication process of the released structure was selected to create a test specimen for a novel thin-film material characterization experiment that functions as either a tensile or interfacial fracture test for thin films on rigid substrates.

A. Test Design

A microfabricated thin-film structure was developed with the dual purpose of testing both thin-film tensile strength and resistance to delamination along the film/substrate interface (see Fig. 5). The design features a patterned thin film on a rigid substrate such that three strips of thin film extend radially outward from a circular central pad. The central pad and a portion of the attached strips are selectively debonded by the removal of an intermediate sacrificial layer. The resulting released film structure features a floating circular pad which is anchored to the substrate by three constant width strips or "legs." The released pad serves as a platform for the subsequent attachment of a loading mechanism. For example, a permanent magnet can be attached onto the central pad using a surface mount epoxy, and the sample with the permanent magnet can be placed in an external magnetic field. With the precise control of the external magnetic field strength, a calibrated magnetic force lifts the permanent magnet and attached central pad and, in the process, imposes a tensile load on the three anchoring film strips. In our ongoing research, we are conducting such noncontact fixtureless magnetic actuation experiments for mechanical characterization of thin films and interfaces. Details of the permanent magnet assembly, experimental test setup, load versus deflection results, data extraction, and analysis are beyond the scope of this paper and will be presented in detail in a different publication. In addition to magnetic actuation, the test sample can be used for mechanical characterization using fixtured nano- or microscale tensile test equipment. For example, if one was to use a nanoindenter, a flat tip is first attached to the released pad using an epoxy, and the tip is then pulled up to get load versus deflection data.

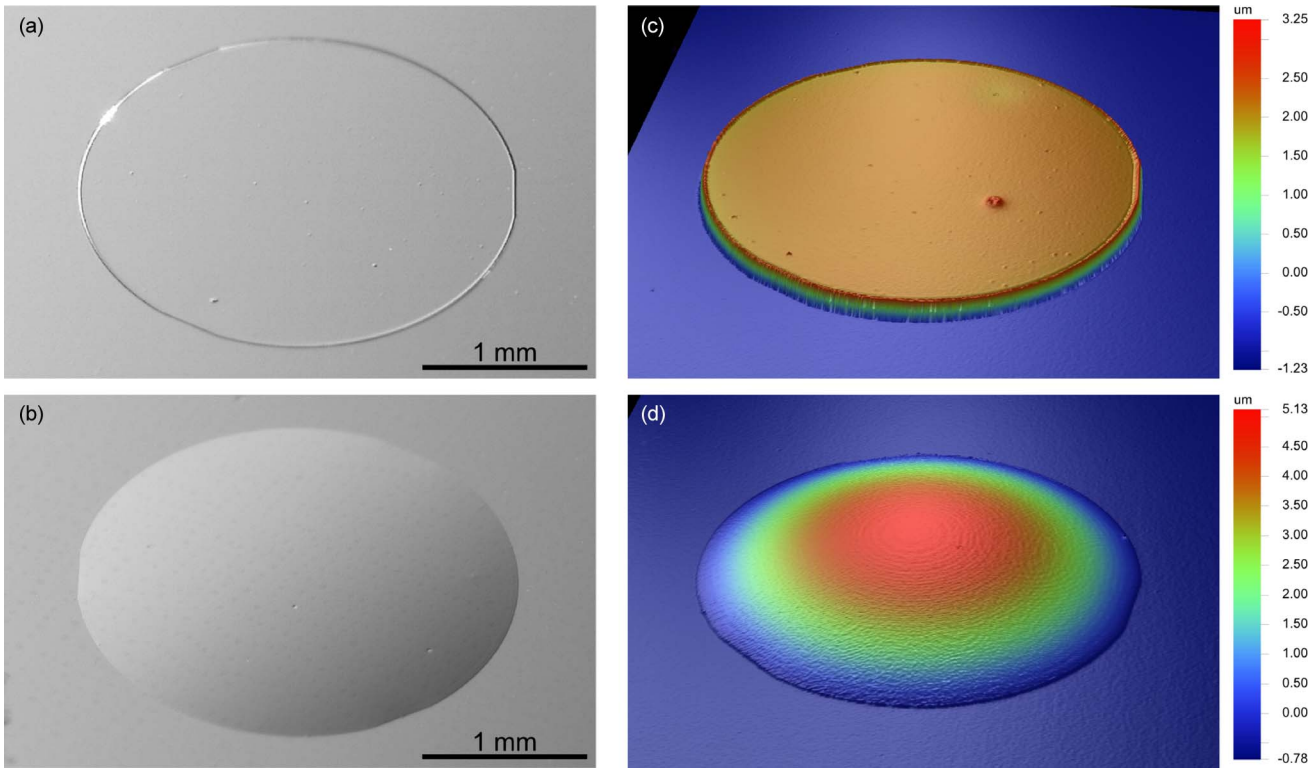

Fig. 4. Cu-coated PPC before and after reflow showing transformation from disk shape to dome shape. (a and b) Optical images taken with Keyence VHX-600 microscope. (c and d) Images generated by Veeco Wyko NT-2000 optical profiler.

TABLE I
DIMENSIONS OF FABRICATED Cu/PPC SPHERICAL DOMES

Planar diameter d (μm)	Initial disc height h_i (μm)	Dome height h_f (μm)	Radius of curvature R (cm)
2190	3.04	5.75	10.4
2680	3.04	5.84	15.4
3670	3.04	5.89	28.6

The vertical compliance of the structure is thus dependent upon the tensile behavior of the attached film strips. With a known vertical force and corresponding measured displacement (and released strip angle), the tensile stress-strain response of the film strips can be determined. When the film/substrate interface is strong, the load can be continuously increased until cohesive failure of the film strips. However, when the film/substrate interface is relatively weak, the vertical force may result in the delamination of the strips from the substrate. In this test mode, the interfacial fracture toughness between the film material and the substrate material can be characterized via a peel test analysis.

Some advantages of using magnetic loading include a fixtureless test design, noncontact actuation, and elimination of some of the practical issues involved with handling the test specimen and applying the load through mechanical means. With the external magnetic field located away from the sample, the sample can be easily placed in temperature/humidity chambers to perform mechanical characterization under various environmental conditions. As most materials in MEMS, microelectronic, and other thin-film systems have weak or negligible magnetic properties, a wide variety of material systems can be tested so that the only magnetic interaction is between the external field and the assembled permanent magnet. In this paper, we focus on the fabrication of the released film test geometry and the integration of the novel doming process described earlier.

B. Sample Preparation

For the test specimens detailed in this work, Cu film strips are fabricated over a natively oxidized silicon substrate. The main steps of fabrication are outlined in Fig. 6: (a) patterning of sacrificial layer; (b) seed metallization; (c) doming of thin metal film; (d and e) patterning of thin-film test strips; and (f) release to define the initially debonded film structure. Fabrication is relatively simple and requires only two photolithography mask steps, and samples can be batch fabricated to produce tens to hundreds of samples on a single wafer. In the mask designs used in this research, the central film pad has a fixed diameter of 1650 μm, the sacrificial disk has a diameter that ranges from 2190 to 3670 μm, and the film strips have widths that range from 25 to 200 μm.

The use of a domed sacrificial layer rather than a flat layer is significant for two reasons: 1) A sharp and shallow precrack as opposed to a stepped profile is created where the film and substrate are initially debonded, and (2) the domed film is more resistant to stiction during the release step as is discussed hereinafter. As was done during reflow characterization, these domes were fabricated with a 500-nm sputtered Cu seed layer over exposed PPC [see Fig. 6(a) and (b)], followed by heating at 100 °C on a hot plate for 5 min [see Fig. 6(c)]. After the reflow process, additional Cu was electroplated up to a final film

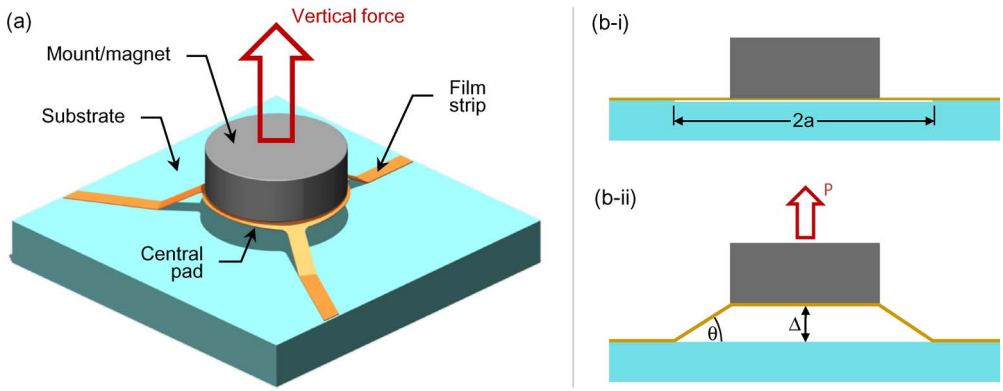

Fig. 5. Thin-film characterization test design. (a) Three-dimensional illustration showing vertical loading of central pad applied through an assembled mount or permanent magnet. Tensile and peeling forces are imposed along the three anchoring film strips. (b) Idealized side view of test specimen showing two anchoring film strips: (i) At rest with initial debonded length $2a$ and (ii) applied vertical loading with force P, displacement Δ, and strip angle θ.

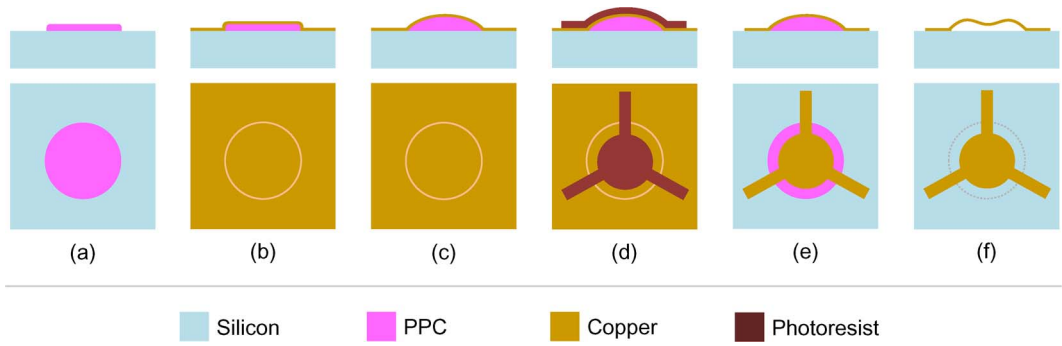

Fig. 6. Fabrication process of test specimen used to characterize the Cu thin-film tensile strength and/or interfacial fracture strength of Cu thin film on Si substrate. The region of the Cu film pattern encompassed by the dotted line in (f) indicates the debonded area.

thickness of 1.5–1.7 μm. Pretreatment in a citric acid/hydrogen peroxide solution was done immediately before plating to remove any surface oxides and ensure a strong bond with the seed layer. Electroplating was done using a standard copper/sulfuric acid electrochemical bath [14] with a phosphorus-doped copper anode. Trace amounts of polyethylene glycol, bis(sodiumsulfopropyl)disulfide, and janus green B were added to the bath as a carrier, brightener, and leveler, respectively, to improve the quality of the copper deposition. The sample was plated at room temperature with no agitation and a current density of 10 mA/cm^2 for a copper electrodeposition rate of 13 μm/min. An AZ-1512 photoresist etch mask was then patterned [see Fig. 6(d)], followed by a subtractive wet etch in diluted Transene APS-100 Cu etchant to define the test film pattern [see Fig. 6(e)]. After etching, the PPC is no longer fully encapsulated by the Cu film, facilitating its removal during the release step.

C. Thermal and Supercritical Release

After the Cu pattern is defined, the underlying PPC dome must be removed in order to release the central pad and strip ends from the substrate. For typical sacrificial materials removed by wet etch, stiction forces can cause the released film features to collapse and re-adhere to the substrate. To overcome stiction effects, two alternative release methods are demonstrated: 1) dry thermal decomposition and 2) wet etch and supercritical dry. The thermal release technique requires baking

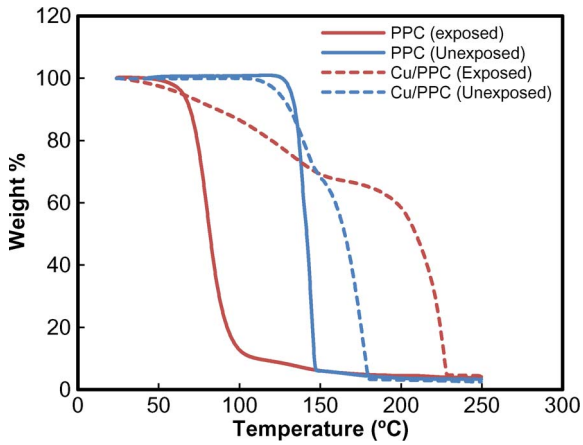

Fig. 7. TGA of exposed/unexposed PPC with and without Cu coating.

the samples at high temperature within a nitrogen-purged oven in order decompose the PPC. The native PPC compound used was observed to decompose rapidly between 80 °C and 140 °C, depending on its exposure level to deep UV. However, much higher oven temperatures were required to decompose the PPC in the fabricated test specimens. A thermal gravimetric analysis (TGA) was performed to characterize this effect of a Cu coating on PPC decomposition (see Fig. 7). The samples were heated at a rate of 0.5 °C/min while weight was measured *in situ*. In both exposed and unexposed cases, the presence of Cu significantly slowed down the rate of PPC decomposition, as temperatures reached as high as 240 °C before all of the exposed PPC had

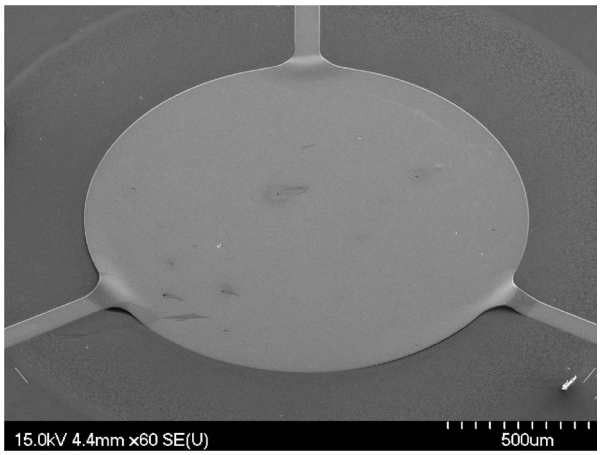

Fig. 8. SEM image showing readhesion of Cu film pattern after PPC decomposition.

decomposed. These findings correlate well with other studies by Kohl et al. [3], [15], which document the effect of inhibited decomposition due to trace amounts of Cu uptake into PPC, and even suggest a chemical interaction between Cu and PPC as the basis of this phenomenon. However, the previous studies cast PPC on a copper substrate. The GBL solvent present in the PPC solution was suggested to have transported the trace amount of Cu from the substrate into the film during soft baking. However, once the solvent dried out, the transportation of Cu was thought to have been stopped. In this paper, the Cu is deposited onto a dry PPC film. This suggests that the PPC/Cu interaction can be transported into the film through dry contact. This could have occurred by implantation of Cu into the film through sputtering and/or trace amounts of residual solvent that might have remained in the PPC.

Test specimens that were fabricated using the thermal release technique were first immersed in IPA to dissolve the photoresist etch mask and then baked at 250 °C for 2 h. Although a handful of specimens were successfully released in this manner, the majority of samples suffered from the relaxation of the thin Cu dome and the readhesion of the central pad to the substrate during the bake process as shown in Fig. 8. While it was expected that the thin flexible Cu film would somewhat collapse upon removal of the underlying PPC, the resulting surface contact often resulted in a strong bond that rendered the specimen unusable for thin-film characterization. The cause of this readhesion is unknown and was problematic for a wide range of bake temperature profiles. For comparison, nondomed samples were also fabricated and baked but achieved no success with all cases suffering from Cu readhesion. The domed samples performed marginally better than the flat ones, most likely because their initially curved surface would warp and ripple during relaxation and limit the available contact area to the substrate. It is expected that lower aspect ratio domes with thicker and stiffer metallized features would be more reliably released using thermal decomposition. However, due to the low yield of samples for the thin-film characterization test and the need for a low-temperature fabrication option, an alternative wet release technique was pursued.

The second method used to release the Cu film features involved dissolving the PPC in solvent followed by supercritical drying. Samples were first immersed in agitated N-methyl-2-pyrrolidone solvent for 24 h to dissolve the PPC, followed by immersion in IPA for another 24 h. The supercritical drying process was done using a Tousimis Autosamdri-815B. During this process, CO_2 is dissolved into the IPA bath, and the chamber conditions are ramped to exceed the fluid critical point of 1072 $\mathrm{lbf/in^2}$ and 31 °C. After reaching supercritical conditions, the chamber is vented at elevated temperature so that the fluid transitions into the gas phase and results in the release of the central Cu pad and film strip ends. The supercritical drying process averts the stiction problems that plague conventional wet release techniques and was shown to be a reliable release process for the fabrication of test specimens. A successfully released sample via supercritical dry is shown in Fig. 9. As mentioned earlier, the initially curved surface above the PPC dome becomes rippled upon removal of the PPC dome due to it being a thin flexible film. However, the resulting degree of waviness is slight, as only a few ripples are formed with heights of less than 10 μm over the entire 2–4-mm span of the released structure. In fact, the SEM image was unable to capture this mild waviness and is hence accompanied by an optical image of the same sample in Fig. 9. Also, the ripples have not been shown to be an issue for the subsequent attachment of a permanent magnet or other loading mechanism. It should be further noted that the pad and the attached magnet are used to transfer the force from the external magnetic field to the three legs of the

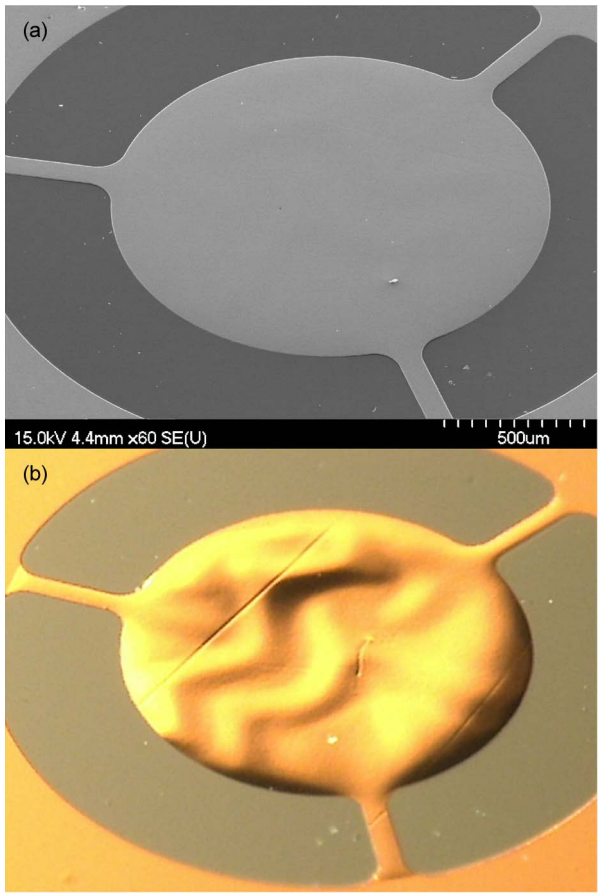

Fig. 9. Released Cu thin-film structure after supercritical drying. The waviness of the released film is too slight to be captured by (a) the SEM but is more visible under (b) an optical microscope.

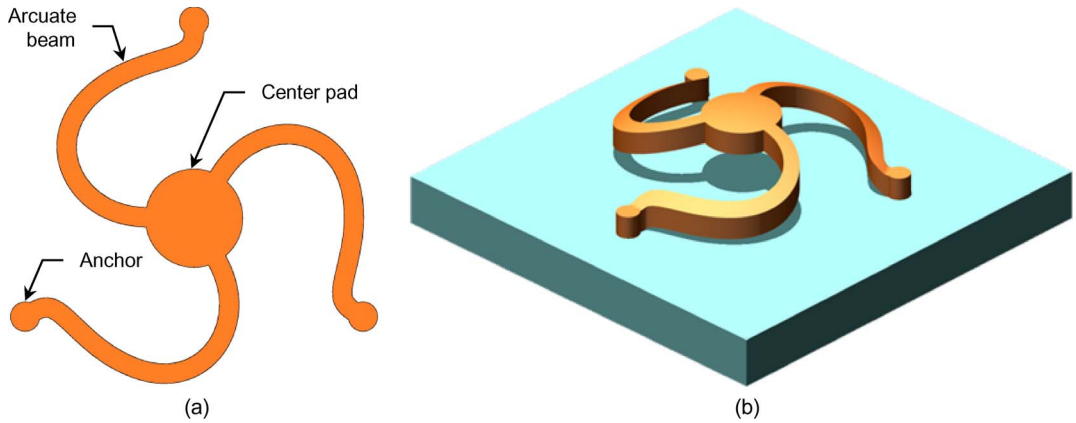

Fig. 10. Domed multipath interconnect design shown as (a) top view and (b) 3-D view on substrate. Similarly as with the thin-film material characterization test, the design features a floating Cu center pad which is anchored to the substrate by three arcuate beams.

test specimen, and thus, the external force is borne by the legs, not by the pad.

IV. Alternative Design

The dome fabrication and release procedures detailed in the development of the thin-film characterization test specimens have several other potential applications. Specifically of interest are domed structures that can have structural and/or electrical applications in a microelectronic package or MEMS sensor. In microelectronic packaging applications, solder balls or solder bumps are commonly used to attach a silicon die to a substrate or a substrate to a board. However, there are several motivations for pursuing compliant interconnects over traditional rigid solder balls. The solder balls tightly couple a silicon chip to an organic substrate of considerable CTE mismatch. Under thermomechanical loading, this mechanical coupling can result in excessive stress near the solder balls and induce cracks in the silicon, dielectric sublayers, intermetallics, or within the solder itself. The common remedy is to employ an epoxy-based underfill material which fills the gap between the solder balls. Although the underfill enhances the reliability of the solder balls, it increases the stresses in the die and can result in the cracking or delamination of on-chip dielectric materials. Furthermore, the underfilling process becomes increasingly challenging as the interconnect size and pitch are further reduced in next-generation packages.

A promising strategy to address these issues and improve the reliability of future packages is to decouple the chip from the substrate by replacing the rigid solder ball with a more compliant interconnect structure. Previous work has shown that designs such as the G-Helix [16], FlexConnect [17], and Sea of Leads (SoL) [9] have much higher compliance than solder balls and can result in packages with decreased chip stresses and increased expected life. However, the fabrication of these interconnects requires several steps and must be simplified before they can be adopted for industrial use. For example, the G-Helix and FlexConnect are freestanding structures that require one or more vertical posts to provide the necessary standoff. On the other hand, the SoL approach incorporates a single arcuate interconnect structure atop a confined air pocket to provide the necessary compliance and mechanical integrity. Thus, the incorporation of reflowed PPC domes into the interconnect design can significantly simplify the fabrication of such compliant structures by eliminating the need for posts or other supporting structures. In addition, the 3-D curvature provides an opportunity for more compliant designs. Here, we present a domed multipath compliant interconnect design and proposed fabrication procedure that is enabled through PPC reflow.

A. Interconnect Design and Fabrication

The proposed interconnect features nonlinear Cu beams that connect to a floating center pad. An example design currently being explored is the domed tripath shown in Fig. 10. The multipath approach can be utilized to reduce electrical parasitics while simultaneously adding mechanical redundancy to the structure in the case of a beam failure. The vertical height of the interconnect structure provides vertical compliance, while the arcuate legs provide compliance in the planar or lateral direction. Thus, the freestanding structure will be able to decouple the die from the substrate in all three orthogonal directions and will reduce the stresses induced in the die under thermal excursions. Also, unlike other interconnects discussed earlier, the proposed interconnects have a periodic symmetry around the center pad, and thus, the die pad and the substrate pad can be vertically aligned during assembly. This design is also well suited for probing applications as the center pad is at the highest point of the interconnect.

The width, thickness, and length of the arcuate structures as well as the height and curvature of the dome can be adjusted to obtain high mechanical compliance and low electrical parasitics such that the proposed interconnects are thermomechanically reliable without compromising the electrical performance of the intended application. The initial target dimensions being considered are beams with a cross section of 4 μm $\times$ 8 μm, dome height of 10 μm, and pitch of 100 μm. With these dimensions, the structure is expected to have sufficient stiffness to maintain a hemispherical shape and provide a compliance of 1–5 mm/N, based on preliminary calculations.

With its nonlinear anchoring legs and more compact dimensions, the domed multipath interconnect is a simple extension of the film characterization test design and likewise involves the same fabrication process as discussed in Section III. A

significant advantage to using the dome is that the entire Cu structure, including the center pad, arcuate beams, and anchors, can be fabricated simultaneously in one step, without the need for separately fabricated posts or other supports. Instead, the structure can be released from the substrate by the removal of the PPC dome, which can be accomplished using a dry thermal or wet supercritical process as demonstrated earlier.

V. Summary

A methodology for microfabricating precisely defined 3-D spherical domes was developed through reflow of a thermally decomposable PPC-based photoresist. The encapsulation of the photoresist with a thin metal film prior to reflow caused the characteristic reflow and decomposition to shift to a higher temperature. Using deep UV-exposed PPC with a thin sputtered metal coating, an optimized one-step reflow bake at 100 °C resulted in a spherical dome with predetermined footprint, height, and curvature.

The use of the encapsulated dome as a suitable sacrificial supporting structure was demonstrated through the fabrication of a patterned and released compliant metal device. Cu was electroplated over the dome and patterned to define specimens for a novel thin-film material characterization test. Subsequent thermal decomposition of the PPC to release the patterned metal film achieved mixed success. While a handful of specimens were sufficiently released for use in the experimental test, the majority of samples suffered from a strong readhesion of the Cu film to the Si substrate. An alternative and more robust release technique involved dissolving the sacrificial polymer in solvent followed by a supercritical dry process in a CO_2/IPA bath.

A significant future application of the PPC dome and release procedures detailed in this work is in the design and fabrication of compliant chip-to-substrate interconnects. The proposed interconnect design is a slight modification of the film characterization test and features domed nonlinear electrical paths connecting to a floating center pad. Such interconnects have potential to increase the reliability of next-generation microelectronic packages.

References

[1] S.-D. Moon, S. Kang, and J.-U. Bu, "Fabrication of polymeric microlens of hemispherical shape using micromolding," *Opt. Eng.*, vol. 41, no. 9, pp. 2267–2270, Sep. 2002.

[2] G. H. Feng, C. C. Sharp, Q. F. Zhou, W. Pang, E. S. Kim, and K. K. Shung, "Fabrication of MEMS ZnO dome-shaped-diaphragm transducers for high-frequency ultrasonic imaging," *J. Micromech. Microeng.*, vol. 15, no. 3, pp. 586–590, Mar. 2005.

[3] V. Rajarathinam, N. Fritz, S. A. B. Allen, and P. A. Kohl, "Imprint lithography enabling ultra-low loss coaxial interconnects," *Microelectron. Eng.*, vol. 88, no. 3, pp. 240–246, Mar. 2011.

[4] C. H. Han and E. S. Kim, "Fabrication of dome-shaped diaphragm with circular clamped boundary on silicon substrate," in *Proc. 12th IEEE Int. Conf. MEMS*, Orlando, FL, 1999, pp. 505–510.

[5] D. H. B. Wicaksono, G. Pandraud, C. K. Yang, J. Dankelman, and P. J. French, "Bio-inspired dome-shape SiO2/SiN membrane as strain-amplifying transducer," in *Proc. Eurosensors XXIII Conf.*, Lausanne, Switzerland, 2009, pp. 770–773.

[6] Y.-S. Lin, C.-T. Pan, K.-L. Lin, S.-C. Chen, J.-J. Yang, and J.-P. Yang, "Polyimide as the pedestal of batch fabricated micro-ball lens and micro-mushroom array category: Micro opto electro mechanical systems," in *Proc. 14th IEEE Int. Conf. MEMS*, Interlaken, Switzerland, 2001, pp. 337–340.

[7] N. Chomnawang and J. B. Lee, "On-chip dome-shape spiral microinductor for high-frequency applications," in *Proc. Smart Struct. Mater. Conf.*, San Diego, CA, 2002, pp. 50–57.

[8] D. A. Fletcher, K. B. Crozier, K. W. Guarini, S. C. Minne, G. S. Kino, C. F. Quate, and K. E. Goodson, "Microfabricated silicon solid immersion lens," *J. Microelectromech. Syst.*, vol. 10, no. 3, pp. 450–459, Sep. 2001.

[9] M. S. Bakir, H. A. Reed, H. D. Thacker, C. S. Patel, P. A. Kohl, K. P. Martin, and J. D. Meindl, "Sea of leads (SoL) ultrahigh density wafer-level chip input/output interconnections for gigascale integration (GSI)," *IEEE Trans. Electron Devices*, vol. 50, no. 10, pp. 2039–2048, Oct. 2003.

[10] T. J. Spencer, P. J. Joseph, T. H. Kim, M. Swaminathan, and P. A. Kohl, "Air-gap transmission lines on organic substrates for low-loss interconnects," *IEEE Trans. Microw. Theory Tech.*, vol. 55, no. 9, pp. 1919–1925, Sep. 2007.

[11] P. J. Joseph, P. Monajemi, F. Ayazi, and P. A. Kohl, "Wafer-level packaging of micromechanical resonators," *IEEE Trans. Adv. Packag.*, vol. 30, no. 1, pp. 19–26, Feb. 2007.

[12] J. P. Jayachandran, H. A. Reed, H. Zhen, L. F. Rhodes, C. L. Henderson, S. A. B. Allen, and P. A. Kohl, "Air-channel fabrication for microelectromechanical systems via sacrificial photosensitive polycarbonates," *J. Microelectromech. Syst.*, vol. 12, no. 2, pp. 147–159, Apr. 2003.

[13] P. J. Joseph, H. A. Kelleher, S. A. B. Allen, and P. A. Kohl, "Improved fabrication of micro air-channels by incorporation of a structural barrier," *J. Micromech. Microeng.*, vol. 15, no. 1, pp. 35–42, Jan. 2005.

[14] M. Schlesinger and M. Paunovic, *Modern Electroplating,* 5th ed. Hoboken, NJ: Wiley, 2010.

[15] T. Spencer, Y.-C. Chen, R. Saha, and P. A. Kohl, "Stabilization of the thermal decomposition of poly(propylene carbonate) through copper ion incorporation and use in self-patterning," *J. Electron. Mater.*, vol. 40, no. 6, pp. 1350–1363, 2011.

[16] Q. Zhu, L. Ma, and S. K. Sitaraman, "Development of G-Helix structure as off-chip interconnect," *J. Electron. Packag.*, vol. 126, no. 2, pp. 237–246, Jun. 2004.

[17] K. Kacker and S. K. Sitaraman, "Electrical/mechanical modeling, reliability assessment, and fabrication of flexconnects: A MEMS-based compliant chip-to-substrate interconnect," *J. Microelectromech. Syst.*, vol. 18, no. 2, pp. 322–331, Apr. 2009.

Gregory T. Ostrowicki received the B.S. degree in mechanical engineering from Rutgers University, Piscataway, NJ, and the M.S. degree in mechanical engineering from the Georgia Institute of Technology (GT), Atlanta. He is currently working toward the Ph.D. degree in mechanical engineering at GT.

His research interests include micromechanics, thin-film adhesion, electronic packaging, microelectromechanical systems, and finite-element analysis.

Nathan T. Fritz received the B.S. degree in chemical engineering from Kansas State University, Manhattan, Kansas, in 2007. He is currently working toward the Ph.D. degree in chemical and biomolecular engineering at the Georgia Institute of Technology, Atlanta.

His current research focuses on materials and processing for air-gap microstructures used in microelectronics. This includes investigations of thermal sacrificial materials, photodefinable POSS dielectrics, and electroless deposition of metals. Advancements to the air gaps will be applied to work on a low-cost MEMS packaging process.

Raphael I. Okereke received the B.S. degree in mechanical engineering from the University of Oklahoma, Norman, OK, and the M.S. degree in mechanical engineering from the Georgia Institute of Technology (GT), Atlanta. He is currently working toward the Ph.D. degree in mechanical engineering at GT.

His research interests are in the areas of MEMS, electronics packaging, and mechanics of materials.

Paul A. Kohl (A'92–M'03) received the Ph.D. degree from the University of Texas, Austin, Texas, in 1978.

He was with AT&T Bell Laboratories, Murray Hill, NJ. In 1989, he joined the faculty of the Georgia Institute of Technology, Atlanta, where he is currently a Regents' Professor and holder of the Thomas L. Gossage/Hercules Inc. Chair. He is also the Director of the Interconnect Focus Center, one of the six Semiconductor Research Corporation Focus Centers sponsored by the DARPA and the semiconductor industry. His research interests are in electronic packaging and interconnect.

Suresh K. Sitaraman received the Ph.D. degree in mechanical engineering from the Ohio State University, Columbus, Ohio, the M.A.Sc. degree in mechanical engineering from the University of Ottawa, Ottawa, Ontario, Canada, and the B.Eng. degree in mechanical engineering from the University of Madras, Chennai, Tamil Nadu, India.

He is currently a Professor with the George W. Woodruff School of Mechanical Engineering, Georgia Institute of Technology (Georgia Tech), Atlanta. Prior to joining Georgia Tech in 1995, he was with the IBM Corporation. His expertise is in the areas of fabrication, characterization, thermomechanical modeling, and reliable design of microscale and nanoscale structures for a wide range of applications. He directs the Computer-Aided Simulation of Packaging Reliability Laboratory at Georgia Tech and has guided a number of postdoctoral fellows, doctoral, masters, and undergraduate students, and high-school interns. He has published extensively in journals and conferences over the years.

Dr. Sitaraman is a Fellow of ASME. He serves as an Associate Editor for the IEEE Transactions on Components, Packaging, and Manufacturing Technology. His coauthored papers won the Commendable Paper Award from the IEEE TRANSACTIONS ON ADVANCED PACKAGING in 2004 and the Best Paper Award from the IEEE TRANSACTIONS ON COMPONENTS AND PACKAGING TECHNOLOGY in 2001 and 2000. He was the recipient of the Sustained Research Award from Georgia Tech-Sigma Xi in 2008 and the Outstanding Faculty Leadership Award for the Development of Graduate Research Assistants from Georgia Tech in 2006. He was also the recipient of the Metro-Atlanta Engineer of the Year in Education Award in 1999, the Outstanding Faculty Education Award from the Packaging Research Center in 1998, and the NSF-CAREER Award in 1997.